

Journal Pre-proof

Fine-tuning of the PAX-SIX-EYA-DACH network by multiple microRNAs controls embryo myogenesis

Camille Viaut, Shannon Weldon, Andrea Münsterberg



PII: S0012-1606(20)30276-1

DOI: <https://doi.org/10.1016/j.ydbio.2020.10.005>

Reference: YDBIO 8326

To appear in: *Developmental Biology*

Received Date: 20 February 2020

Revised Date: 6 October 2020

Accepted Date: 14 October 2020

Please cite this article as: Viaut, C., Weldon, S., Münsterberg, A., Fine-tuning of the PAX-SIX-EYA-DACH network by multiple microRNAs controls embryo myogenesis, *Developmental Biology* (2020), doi: <https://doi.org/10.1016/j.ydbio.2020.10.005>.

This is a PDF file of an article that has undergone enhancements after acceptance, such as the addition of a cover page and metadata, and formatting for readability, but it is not yet the definitive version of record. This version will undergo additional copyediting, typesetting and review before it is published in its final form, but we are providing this version to give early visibility of the article. Please note that, during the production process, errors may be discovered which could affect the content, and all legal disclaimers that apply to the journal pertain.

© 2020 Published by Elsevier Inc.

Fine-tuning of the Pax-Six-Eya-Dash network by multiple microRNAs controls embryo myogenesis

Camille Viaut^{1,2}, Shannon Weldon¹ and Andrea Münsterberg^{1,*}

¹ School of Biological Sciences, Cell and Developmental Biology, University of East Anglia, Norwich Research Park, Norwich, NR4 7TJ, UK

² Present address: Université de Paris, Institut Cochin, INSERM, CNRS, F-75014 PARIS, France

* Corresponding author:

Email: A.Munsterberg@uea.ac.uk

Phone: +441603592232

Keywords: miR-128, myomiRs, chicken embryo, somite myogenesis, PSED network, EYA4

Running title: miR-128 regulates PSED in myogenesis

Abstract

MicroRNAs (miRNAs), short non-coding RNAs, which act post-transcriptionally to regulate gene expression, are of widespread significance during development and disease, including muscle disease. Advances in sequencing technology and bioinformatics led to the identification of a large number of miRNAs in vertebrates and other species, however, for many of these miRNAs specific roles have not yet been determined. LNA *in situ* hybridisation has revealed expression patterns of somite-enriched miRNAs, here we focus on characterising the functions of miR-128. We show that antagomiR-mediated knockdown (KD) of miR-128 in developing chick somites has a negative impact on skeletal myogenesis. Computational analysis identified the transcription factor EYA4 as a candidate target consistent with the observation that miR-128 and *EYA4* display similar expression profiles. Luciferase assays confirmed that miR-128 interacts with the *EYA4* 3'UTR. *In vivo* experiments also suggest that *EYA4* is regulated by miR-128. EYA4 is a member of the PAX-SIX-EYA-DACH (PSED) network of transcription factors. Therefore, we identified additional candidate miRNA binding sites in the 3'UTR of *SIX1/4*, *EYA1/2/3* and *DACH1*. Using the miRanda algorithm, we found sites for miR-128, as well as for other myogenic miRNAs, miR-1a, miR-206 and miR-133a, some of these were experimentally confirmed as functional miRNA target sites. Our results reveal that miR-128 is involved in regulating skeletal myogenesis by directly targeting *EYA4* with indirect effects on other PSED members, including *SIX4* and *PAX3*. Hence, the inhibitory effect on myogenesis observed after miR-128 knockdown was rescued by concomitant knockdown of *PAX3*. Moreover, we show that the PSED network of transcription factors is co-regulated by multiple muscle-enriched microRNAs.

Introduction

In vertebrates, most of the axial skeleton and all skeletal muscles of the trunk and limbs are derived from somites, transient metameric structures generated along the anterior-posterior axis by segmentation from the pre-somitic mesoderm (PSM) (Christ and Ordahl, 1995). Subsequent specification of cell fates within somites and the differentiation of a somite into sclerotome, dermomyotome and myotome depends on interactions with surrounding tissues, which are the source of extrinsic molecular signals. These signals include WNT proteins derived from the dorsal neural tube and surface ectoderm, bone morphogenetic proteins (BMP) from the lateral plate mesoderm, and Sonic hedgehog (SHH) from the notochord and floor plate of the neural tube (Brent and Tabin, 2002; Yusuf and Brand-Saberi, 2006; Christ, Huang and Scaal, 2007).

Myogenesis starts in the dermomyotome and requires the commitment of a pool of cells into the skeletal muscle lineage. The first molecular markers characterising myogenic precursors are the paired-box transcription factors PAX3 and PAX7 (Kassar-Duchossoy *et al.*, 2005; Relaix *et al.*, 2005), which support the proliferation and survival of myogenic progenitors before differentiation (Buckingham and Relaix, 2007). In both mouse and chicken embryos, PAX3/7 activate and control the expression of the genes encoding myogenic regulatory factors (MRF), such as MYF5 and MYOD1 (Williams and Ordahl, 1994; Maroto *et al.*, 1997; Tajbakhsh *et al.*, 1997; Bajard *et al.*, 2006). Furthermore, mice lacking both PAX3 and PAX7 display major defects in myogenesis, suggesting that together these genes are required for normal muscle development (Relaix *et al.*, 2005).

The expression of PAX3/7 is regulated by the activity of members of SIX, EYA and DACH families (Heanue *et al.*, 1999; Grifone *et al.*, 2005). Together these proteins comprise the PSED network, which plays key regulatory roles in the development of numerous organs and tissues such as kidney, ear and muscle (Relaix and Buckingham, 1999). The biochemical interactions and complex feedback loops between PSED members have been dissected (Kumar, 2009). In paraxial mesoderm, the expression of PSED members (PAX1/6/7/9, SIX1/2, EYA2) is upregulated during the transition from presegmented mesoderm to epithelial somites (Mok *et al.*, 2020). In addition, SIX1/4, EYA1/2/4 and DACH1/2 have been shown to initiate myogenesis through activation of the MRF genes, similar to PAX3 and PAX7 (Maroto *et al.*, 1997; Tajbakhsh *et al.*, 1997; Spitz *et al.*, 1998; Heanue *et al.*, 1999; Berkes and Tapscott, 2005; Relaix *et al.*, 2005, 2013; Grifone *et al.*, 2007). Thus, the PSED network is upstream of the genetic regulatory cascade that directs dermomyotomal progenitors toward the myogenic lineage.

SIX family transcription factors are characterised by the presence of two conserved domains, a homeodomain (HD) that binds to DNA, and an amino-terminal SIX domain (SD) that interacts with coactivators (EYA) or corepressors (DACH) of transcription. EYA proteins

are unique co-transcription factor phosphatases. They comprise a C-terminal EYA domain (ED), responsible for interactions with SIX and DACH, and threonine and tyrosine phosphatase activity, which may inhibit DACH corepressor function (Li *et al.*, 2003; Rayapureddi *et al.*, 2003; Tootle *et al.*, 2003). Furthermore, EYA recruits RNA polymerase II and coactivators, such as CREB-binding protein (CBP), or corepressors, such as histone deacetylase (HDAC), to the SIX complex (Li *et al.*, 2003; Jemc and Rebay, 2007).

It has been shown that microRNAs, small non-coding RNAs that regulate gene expression post-transcriptionally (Bartel, 2004, 2009, 2018), are important for embryo myogenesis (Mok, Lozano-Velasco and Münsterberg, 2017). We showed that members of the miR-1/miR-206 and the miR-133 families, which are derived from bi-cistronic primary transcripts, are expressed in the myotome of developing somites where their expression is induced by MRFs (Sweetman *et al.*, 2006, 2008; Goljanek-Whysall *et al.*, 2011). AntagomiR-mediated knockdown (KD) approaches *in vivo* revealed that miR-206 is crucial for the myogenic progenitor to committed myoblast transition by negatively regulating expression of PAX3. PAX3 is initially expressed throughout the somite (Williams and Ordahl, 1994), subsequently becomes restricted to the dermomyotome and then to the epaxial and hypaxial dermomyotome. PAX3 is finally downregulated as progenitor cells enter myogenesis. Furthermore, we showed that miR-133 and miR-1/206 directly target BAF60a and BAF60b, thereby affecting the subunit composition of the BAF/BRG1 chromatin remodelling complex (Goljanek-Whysall *et al.*, 2014). This is important to stabilise the myogenic differentiation programme in developing somites. In addition, miR-133 is involved in regulating Sonic Hedgehog pathway activity via negative regulation of GLI3 repressor and this is required for myogenic fate specification as well as somite epithelialisation, proliferation and growth (Mok *et al.*, 2018).

Here we focus on miR-128, which we found enriched in developing somites (Ahmed *et al.*, 2015). miR-128 is intronic and embedded into two distinct genes: *R3HDM1* (R3H domain containing 1) and *ARPP21* (cyclicAMP regulated phosphoprotein 21 kDa) (Bruno *et al.*, 2011), located on chromosomes 7 and 2 in chicken. Both miR-128-1 and miR-128-2 precursors generate the identical mature miRNA. First identified in mouse, miR-128 is enriched in brain, during development and in the adult (Lagos-Quintana *et al.*, 2002); similar observations were made in chicken and zebrafish (Xu *et al.*, 2006; Kapsimali *et al.*, 2007). Furthermore, during cardiac regeneration in newt, miR-128 regulates the expression of the transcription factor *Islet1* (Witman *et al.*, 2013). In chicken, miR-128 expression in the developing heart appears to be limited to a short time-window as it is only seen in stage HH13 embryos (Darnell *et al.*, 2006). As well as being involved in neuronal and cardiac development, miR-128 expression was also detected in adult mouse muscle (Sempere *et al.*, 2004), adult and embryo porcine skeletal muscle (Zhou *et al.*, 2010), and adult and embryo chicken skeletal muscle (Darnell *et al.*, 2006; Lin *et al.*, 2012; Abu-Elmagd *et al.*, 2015). In

mouse, the inhibition of insulin receptor substrate 1 (IRS1) by miR-128 leads to inhibition of myoblast proliferation and induction of myotube formation (Motohashi *et al.*, 2013). In addition, miR-128 promotes myotube formation by targeting myostatin (MSTN), a negative regulator of myogenesis and muscle growth (Shi *et al.*, 2015). These authors also showed that miR-128 inhibited proliferation of mouse C2C12 myoblasts and promotes differentiation and myotube formation. The functions of miR-128 in embryo myogenesis are less well understood. We identify *EYA4* as a novel target for miR-128 and show cooperative effects with miR-206. Using luciferase reporter assays we examine the regulation of additional PSED members by miR-128, as well as by other muscle-enriched microRNAs, including miR-1, miR-206 and miR-133. We show that antagomiR-mediated knockdown (KD) of miR-128 in chick somites inhibits myogenesis and correlates with the deregulation of PSED members, including the derepression of *EYA4* and secondarily the elevated expression of *SIX1/4* genes and *PAX3*. Electroporation of *EYA4* into chick somites inhibits myogenesis, thus mimicking the miR-128 KD phenotype. In miR-128 KD somites myogenesis is restored by inhibition of *PAX3* using an antisense oligonucleotide. Together our findings suggests that microRNA-mediated regulation of the PSED network contributes to the fine-tuning of skeletal muscle development in vertebrate embryos.

Results

Expression of miR-128 overlaps with *EYA4* in the myotome

To analyse the properties of miR-128 during somite development in chick embryos, we determined its spatio-temporal expression profile by whole-mount *in situ* hybridisation (WISH) and cryosectioning (Fig. 1D). At HH11-12, miR-128 was found in the neural tube, developing somites and in the notochord (Fig. 1Di-i'). At HH16-17, miR-128 was detected in the myotome, with no expression apparent in the notochord and weak expression in the dorsal neural tube (Fig. 1Dii-ii''). At HH21-22, miR-128 was found in the branchial arches, around the eye and in fore- and hind limbs (Fig. 1Diii-iii''). Interestingly, miR-128 expression in the chick myotome is similar to the well-known and conserved myomiRs: miR-1, miR-133a/b and miR-206 (Fig. 1A-C) (Sweetman *et al.*, 2008; Ahmed *et al.*, 2015).

To determine possible targets of miR-128 we used TargetScan (release 7.2; March 2018); this generated a list of 439 potential target genes. The molecular functions of miR-128 predicted targets was determined using GO term and g:GOSt analyses (Fig. 2A). The GO term annotation showed that 69.2% of miR-128-predicted targets were classified as 'cellular process'. Other enriched GO terms included 'biological regulation' (55.3%) and 'developmental process' (28.8%). The g:GOSt analysis performed using g:Profiler showed similar results for broad categories. However, a larger number of targets were classified as playing a role in 'developmental process'. The miR-128 targets listed in this category from GOTERM_BP_1 and g:GOSt were compared and 126 targets were common between the

two different tools (Fig. 2B). Of these 120 targets more than 50% were found in the brain (65), which is notable as miR-128 was described as brain-enriched, about 10% were found in the eye (12), 8% in muscle (10) and less than 2% in the heart (2) (Fig. 2C).

One of the ten predicted targets for miR-128 in muscle was *EYA4* (Fig. 2D), a member of the PAX-SIX-EYA-DACH (PSED) network of transcriptional regulators, which act upstream of the MRFs in myogenesis. Like the other members of this network, EYA4 proteins have been highly conserved across species during evolution (Fig. 2E, F). Interestingly, Gga-EYA4 shares a higher percentage of identity with its human, mouse, and *Xenopus* orthologous (Hsa-EYA4, Mmu-Eya4, Xla-eya4) (Fig. 2E), than with its homologous Gga-EYA1, Gga-EYA2, and Gga-EYA3 (Fig. 2F). This is particularly true in the EYA domain localised in the C-terminal region; this domain being common to all the EYA family members.

To examine a possible interaction between miR-128 and *EYA4* we characterised the expression profile of *EYA4* by whole-mount *in situ* hybridisation (WISH) (Fig. 1E). At HH11-12, *EYA4* was mainly expressed in neural folds in the head region and in some cranial placodes, such as the optic and otic vesicles (Fig. 1Eiv). *EYA4* was also expressed in a region proximal to the inflow region of the heart. At this stage no expression was detected in somites (Fig. 1Eiv'). As the embryo developed, *EYA4* transcripts were detected in the branchial arches and somites. From HH16, *EYA4* was seen in the myotome with stronger expression at HH21-22 in the dorsomedial lip of the dermomyotome (Fig. 1Ev-vi''). *EYA4* transcripts were also detected in dorsal root ganglia and in a posterior region of the developing limbs (Fig. 1Evi). Thus, expression of miR-128 and *EYA4* was overlapping in the myotome and limb buds. We therefore examined whether miR-128 regulates *EYA4* expression post-transcriptionally and tested whether a direct interaction could be confirmed.

Luciferase assays confirm negative regulation of *EYA4* by miR-128

To validate a potential interaction of miR-128 with the 3'UTR of *EYA4* (Fig. 3A), we generated luciferase reporters, both wild-type (WT) constructs and constructs where the miR-128 target site was mutated (mut). A potential miR-128 site was predicted in the 5' part of the 3'UTR sequence by TargetScan and MiRanda algorithms; miR-27b has the same seed sequence as miR-128 and is predicted to target the same site (Fig. 3A, B). Additional candidate target sites in the *EYA4* 3'UTR included sites for miR-1a and miR-206, which have the same seed, as well as miR-133 (Fig. 3A, B; Fig. 4B). It has been found that miRNA sites located at the 5' and 3' extremities of a 3'UTR sequence are more likely to be functional (Long *et al.*, 2007; Ekimler and Sahin, 2014). Therefore, it is noteworthy that all these sites are located within the first 1,000 bp of the *EYA4* 3'UTR sequence, which is 6,000 bps in total. A 1kb fragment was cloned into a luciferase reporter and mutant constructs were generated for miR-27b/128, miR-1a/206 and miR-133a. Base pairing between the microRNAs and the putative target sites are shown and the mutated nucleotides are indicated (Fig. 3B; Fig. 4B).

In luciferase assays co-transfection of miR-128 mimics with the *EYA4* 3'UTR lead to a decrease in relative luciferase activity compared to control (siC) (68% activity; t-test: $p < 0.001$). Luciferase activity was restored to 93.5% of control by mutating miR-128 binding site (Fig. 3C). Co-transfection of miR-206 mimics also regulated the *EYA4* 3'UTR. A decrease in luciferase activity was observed (76% activity; t-test: $p < 0.001$), which was restored by mutating miR-206 site (92.5% activity) (Fig. 3D). Interestingly, miR-27b did not affect luciferase expression suggesting it does not interact with the *EYA4* 3'UTR (Fig. 3F). Similarly, miR-1a did not interact with the *EYA4* 3'UTR (Fig. 3G) even though it shares the same seed sequence with miR-206. This indicates that miR-target gene interactions are not only based on complementarity between the seed and 3'UTR sequences and that additional nucleotides mediate specificity and need to be taken into account. Co-transfection of miR-133 mimic with the *EYA4* 3'UTR reporter had no effect (Fig. 4E).

Seed sequences are short (6-8 nts), and miRNAs often regulate several hundred targets. Conversely, multiple miRNAs can regulate the expression of a single gene by targeting different sites on the 3'UTR of its mRNA (Selbach *et al.*, 2008; Bartel, 2009, 2018). Because miR-128 and miR-206 led to a decrease in luciferase activity of the *EYA4* 3'UTR reporter we examined whether they cooperate. As before, luciferase activity was decreased in response to transfection of miR-128 mimic alone or miR-206 mimic alone (by 28.5% or 21.8%, Fig. 3E). This was very similar to the decreases observed in the previous experiments (32% or 24%, Fig. 3C, D). Smaller decreases in luciferase activity were observed with half the concentration of miR-128 or miR-206 mimic (mixed 1:1 with control mimic to give the same final concentration of oligo), 14.6% and 11% respectively. However, when miR-128 and miR-206 mimics were co-transfected expression of the *EYA4* 3'UTR luciferase reporter was reduced by 40.4% (Fig. 3E). Thus, their combined effect is greater than the sum of their individual effects, suggesting that miR-128 and miR-206 can act together to regulate *EYA4* expression (Ivanovska and Cleary, 2008; Lu and Clark, 2012).

Members of the PSED network are regulated by myogenic microRNAs

Next, we investigated potential miRNA-mediated regulation of other members of the PSED network: *EYA1/3*, *SIX1/4* and *DACH1*. Using TargetScan and miRanda, several miRNAs were identified and predicted to target PSED members (Suppl. Table 1). Here, we focused on miR-128, miR-1/206 and miR-133 (Table 1; Figs. 3, 4 and 5). Fragments of the 3'UTRs were cloned to generate luciferase reporter constructs, and mutations were introduced into the putative miRNA sites.

We examined *EYA1* and *EYA3*, two additional EYA family members with putative target sites in their 3'UTRs (Fig. 4A, B, F). Luciferase reporter assays confirmed that miR-133 targets both *EYA1* and *EYA3*, but not *EYA4* (Fig. 4C-E). Specifically, luciferase activity of *EYA1* 3'UTR reporter was decreased by 26.6% (73.4% activity; t-test: $p < 0.001$) in response

to miR-133a mimic. This was restored by mutating the miR-133 site with relative luciferase activity going back to 94% (Fig. 4C). Luciferase reporter activity of *EYA3* 3'UTR decreased by 21.7% (78.3% activity; t-test: $p < 0.001$) in response to miR-133a mimic. This was restored to 97.3% activity after mutation of miR-133 site (Fig. 4D). No effect on luciferase activity was observed using the *EYA4* 3'UTR reporter (Fig. 4E).

In addition, *EYA1* is regulated by miR-128 via two independent sites in the 3'UTR (Fig. 4F, G). With both putative target sites (TS) present in the *EYA1* 3'UTR, a decrease of 34% of the luciferase activity was observed in response to miR-128 mimic (66% activity). Mutation of each site individually (TS1, TS2) only partially restored luciferase activity levels, to 73% and 83% respectively. However, mutation of both sites restored luciferase activity to 94%. This shows that both TS1 and TS2 can work independently with TS2 being slightly more effective. Interestingly, the *EYA1* 3'UTR did not respond to miR-27b mimic.

Other members of the PSED network are *SIX1*, *SIX4* and *DACH1* and whilst there was no predicted target site for miR-128 in their 3'UTRs, TargetScan and miRanda predicted sites for miR-1a/206, miR-133 and miR-499 (Fig. 5A, B). Luciferase reporter assays showed a decrease in luciferase activity after transfection of mimics for either miR-1a or miR-206. For all genes, *SIX1/4* and *DACH1*, the effect of miR-206 was stronger compared to miR-1. Specifically, relative luciferase activity of the *SIX1* 3'UTR reporter decreased by 18.2% with miR-1 and by 31.4% with miR-206. For the *SIX4* 3'UTR reporter we observed a decrease of 24.3% with miR-1 and 37.2% with miR-206 (Fig. 5C, D). The *SIX4* 3'UTR reporter did not respond to miR-133 mimic (Fig. 5D), or to miR-499 mimic (not shown).

The *DACH1* 3'UTR reporter contained two predicted target sites for miR-1a and miR-206. Transfection of mimics for these microRNAs led to a decrease of 35% and 45.4% in luciferase activity, respectively. Introducing point mutations into the miR-1a/206 sites separately only led to a minor rescue of luciferase activity to 74% and 59% activity, respectively (t-test: $p < 0.001$) (Fig. 5E), suggesting that the two sites can work independently. Mutation of both sites restored luciferase activity to approximately 90%.

Myogenesis is impaired after miR-128 knockdown and the PSED network - including *EYA4* - is deregulated.

Given the restricted expression of miR-128 in the somite myotome, we asked whether miR-128 is required for myogenesis *in vivo*. In addition, we determined whether miR-128 loss-of-function had an effect on expression of the PSED network and in particular on *EYA4* (Fig. 6). The most posterior six somites of HH14-15 chicken embryos were injected with antagomiR-128 (AM-128), or AM-128 and AM-206 or with a scrambled antagomiR (AM-scr). The resulting phenotypes were assessed after 24 hours using whole-mount *in situ*

hybridisation and cryosections (Fig. 6A-C) or RT-qPCR (Fig. 6D-E). Non-injected contralateral somites were used as additional controls.

AntagomiR-mediated KD of miR-128 led to decreased *MYOD1* expression in developing somites. This was clearly visible in whole mount (Fig. 6Aiv). Cryosections confirmed the loss of *MYOD1* transcripts detected in the myotome (Fig. 6Bxii). Grouping the ISH results showed that the majority of embryos (73.2%) had either complete (n=13/41, 32%) or partial loss of *MYOD1* (n=17/41, 41%) (Fig. 6C). The qualitative ISH data was confirmed by RT-qPCR of dissected somites, which were pooled from seven independent injection experiments. This also showed a reduction of *MYOD1* expression (Fig. 6D).

Interestingly, miR-128 KD led to a concomitant increase in expression of the pre-myogenic transcription factor and PSED member, *PAX3*, which showed an increase in the dermomyotome, especially in its central part where its expression is usually weak (Fig. 6Aiii, 6Bxi). The majority of embryos (70.8%) showed an increase of *PAX3*, 14/24 embryos were similar to the embryo shown (Fig. 6Aiii, 6Bxi), 3/24 showed a partial increase and 7 embryos showed no change (Fig. 6C). A relative increase in *PAX3* transcript levels (30%) after AM-128 injection into somites was confirmed by RT-qPCR (1.3-fold change; t-test: $p < 0.01$) (Fig. 6D). This indicates that myogenic cells in the dermomyotome remained in a progenitor stage of development and did not activate the differentiation programme (Goulding, Lumsden and Paquette, 1994; Williams and Ordahl, 1994; Gros, Scaal and Marcelle, 2004).

In whole-mount embryos, expression of *EYA4*, a validated direct target of miR-128, did not seem to be different between AM-128 injected and non-injected sides (Fig. 6Ai). However, transverse cryosections showed that *EYA4* expression was increased in the central part of the myotome after miR-128 KD (Fig. 6Bix). This phenotype was observed in 51.5% of the embryos: 13/66 were similar to the embryo shown, 21/66 embryos showed partial de-repression (31.8%) and in 48.5% of the embryos (n=32) no change in expression was detectable on the injected side compared to the non-injected side (Fig. 6C). RT-qPCR confirmed the increase in *EYA4* expression, which was 1.4-fold higher in pooled somites injected with AM-128 compared to non-injected pooled somites from the opposite side (t-test: $p < 0.01$) (Fig. 6D). Thus, ISH and RT-qPCR showed that KD of miR-128 resulted in de-repression of *EYA4* expression in the myotome. This is consistent with the *in vitro* luciferase reporter experiments (Fig. 3B, C) and identifies *EYA4* as a direct miR-128 target *in vivo*.

To investigate further the potential combined action of miR-128 and miR-206 on *EYA4* 3'UTR observed by luciferase assays (Fig. 3E), we co-injected AM-128 and AM-206 into somites as before. RT-qPCR of pooled somites from multiple embryos showed that *EYA4* and *PAX3* relative expression levels are equal or higher after co-injection of AM-128 and AM-206 compared to somites injected with either AM128 or AM-206 alone (Fig. 6E).

To examine potential effects of miR-128 KD on other members of the PSED network we used RT-qPCR to assess the expression of *EYA1*, *EYA2*, *EYA3*, *SIX1*, *SIX4* and *DACH1*

(Fig. 6D). In addition, we performed WISH for *SIX4* (Fig. 6A, B). The expression of *EYA1* was 1.2-fold higher than the control, but *EYA2* and *EYA3* were not affected after AM-128 injection (Fig. 6D). The increase of *EYA1* is consistent with luciferase reporter assays, which identified *EYA1* as a direct target for miR-128 *in vitro* (Fig. 4F, G). Although *SIX1* and *SIX4* were not predicted as direct targets of miR-128, a 1.3-fold increase in their expression levels was observed after AM-128 injection, most likely due to indirect effects (Fig. 6D). ISH performed on AM-128 injected embryos also showed an increase in *SIX4* expression in injected somites, in the dorsomedial lip of the dermomyotome and the myotome (Fig. 6Aii, 6Bx). This was observed in 14/25 embryos (56%) (Fig. 6C). These results are consistent with a potential indirect effect and cross-regulation between SIX and EYA co-factors, which have been shown to form a strong complex that activates SIX target genes.

Next, we asked whether targeted mis-expression of *EYA4* would mimic the miR-128 KD phenotype. A pCA β -*Gga-EYA4*-full-length expression construct was injected and electroporated into posterior somites of HH14-15 chicken embryos. After 24h, embryos were harvested; successfully electroporated somites (GFP⁺) and non-injected contralateral somites were dissected for RT-qPCR (Fig. 6F). This confirmed a 1.53-fold increase in *EYA4* expression and a concomitant 1.54- and 1.44-fold increase of *SIX4* and *PAX3* expression (n=7-9; t-test: p<0.001 and p<0.0001, respectively). This correlated with 0.8-fold decrease of *MYOD1* expression (n=6; t-test: p<0.05).

Finally, we examined whether knockdown of *PAX3* expression using a previously validated antisense morpholino could restore the antagomiR-128-induced loss of *MYOD1* expression. We co-injected FITC-labelled *PAX3* morpholino (*PAX3-MO*) or scrambled morpholino (*MO-scr*) with AM-128 into the six most posterior somites of HH13-14 embryos, followed by electroporation (Fig. 6G). *In situ* hybridisation showed a rescue of *MYOD1* expression in the somites that received *PAX3-MO* and AM-128 (Fig. 6Gii, ii'). In embryos co-injected and electroporated with the control *MO-scr* and AM-128, the loss of *MYOD1* was not rescued (Fig. 6Gi, i').

Therefore, elevated expression of *EYA4*, either due to miR-128 KD or due to plasmid electroporation led to deregulation of the PSED network, including *PAX3*, and correlates with the inhibition of myogenesis *in vivo*. This suggests that fine-tuning the expression of *EYA4* in the myotome by miR-128 contributes to control entry into the myogenic programme (Fig. 6H).

Discussion

The MRFs control entry into the myogenic programme, which leads to the formation of skeletal muscle. Upstream of this obligatory step other transcription factors, including the PSED network, direct cells toward myogenesis. Therefore, members of this regulatory network, PAX, SIX, EYA and DACH are referred to as pre-myogenic factors. In vertebrates, *SIX1/4*, *EYA1/2/4*, and *DACH1/2*, have overlapping expression patterns in the myogenic

precursor cells in the somites, in the dermomyotome and the myotome. At limb level, together with PAX3, they play a crucial role in ensuring that migrating myogenic precursor cells remain committed to their fate until they reach their final destination (Christ and Ordahl, 1995).

Experiments in mice and chicken provided insight into the roles of PSED members upstream of the activation of the myogenic programme. Ectopic expression of PAX3, SIX or EYA in chicken embryos led to activation of PAX3 and MRFs (Maroto *et al.*, 1997; Heanue *et al.*, 1999). While in *PAX7*^{-/-} mutant mice skeletal muscle forms normally (Mansouri *et al.*, 1996), *PAX3*^{-/-} mutants have abnormal myotome formation, trunk muscle defects and absence of limb muscle (Bober *et al.*, 1994; Goulding, Lumsden and Paquette, 1994). Moreover, *PAX3*^{-/-}/*PAX7*^{-/-} double-mutant mice have major defects in myogenesis (Relaix *et al.*, 2005). Similarly, no developmental defects were observed in *SIX4*^{-/-} and *EYA2*^{-/-} mice (Ozaki *et al.*, 2001; Grifone *et al.*, 2007), but *SIX1*^{-/-} and *EYA1*^{-/-} mutant mice have important muscle deficiencies (Laclef *et al.*, 2003; Ozaki *et al.*, 2004; Grifone *et al.*, 2007), while *SIX1*^{-/-}/*SIX4*^{-/-} and *EYA1*^{-/-}/*EYA2*^{-/-} double-mutant mice lack all muscles derived from the hypaxial dermomyotome. *SIX1*^{-/-}/*SIX4*^{-/-}/*MYF5*^{-/-} triple-mutant mice display a similar phenotype to what was observed in *PAX3*^{-/-}/*MYF5*^{-/-} mutants, with no expression of *MYOD* and no skeletal muscle formed (Tajbakhsh *et al.*, 1997; Giordani *et al.*, 2007; Relaix *et al.*, 2013), suggesting that SIX and EYA are upstream of PAX.

Transcription regulation of target genes by SIX proteins requires cooperative interaction with EYA proteins (Ohto *et al.*, 1999), moreover SIX1/4 binding to EYA1/2 in the cytoplasm precedes translocation into the nucleus. SIX, often associated with DACH, has been described as a repressor or weak activator, however, when interacting with EYA, the complex formed becomes a strong activator, which is then able to activate SIX target genes, such as *PAX3* and *MYOD1* and therefore influence myogenic differentiation (Heanue *et al.*, 1999; Grifone *et al.*, 2005). In addition, it has also been shown that SIX/EYA complex can directly up-regulate *MYOD* and *MYOG* expression by targeting enhancer elements on their respective promoters (Spitz *et al.*, 1998; Tapscott, 2005; Giordani *et al.*, 2007). These results are consistent with the severe decrease of *MYF5* and *MYOD1* expression, in the myotome, observed in the *SIX1*^{-/-}/*SIX4*^{-/-} double-mutant mice (Grifone *et al.*, 2005; Buckingham and Rigby, 2014).

Here we demonstrate the co-regulation of PSED members by multiple microRNAs that are known to be enriched in skeletal muscle (Mok, Lozano-Velasco and Münsterberg, 2017). In particular, antagomiR-mediated KD of miR-128 inhibits myogenesis, *MYOD1* expression is lost on the injected side and expression of the premyogenic genes, *PAX3*, *SIX4* and *EYA4*, is increased (Fig. 6A, B, D). We propose that the inhibition of myogenesis results from de-repression of *EYA4*, which we show is directly targeted by miR-128 via a site in the 3'UTR (Fig. 3A, B, C). More *EYA4* would lead to formation of transcriptional complexes with SIX

proteins (*SIX1/4*) and to increased expression of *PAX3*, thus keeping cells in a pre-myogenic state. Deregulation of *EYA4* *in vivo*, in developing somites, also affects expression of other members of the PSED network as shown by RT-qPCR (Fig. 6D). The observed increase in *PAX3* expression is consistent with the fact that *PAX3* is a known target of *SIX* (Grifone *et al.*, 2005). Interestingly, a miR-128 site was predicted by TargetScan in the human *PAX3* 3'UTR. Thus, it is possible that *PAX3* is a direct target of miR-128 in human, however, a canonical target site (Bartel, 2009) was not identified in the chicken *PAX3* 3'UTR by any of the algorithms we used in this work.

Overexpression of *EYA4* could phenocopy the miR-128 KD (Fig. 6F). This is consistent with the idea that *EYA4* is an important miR-128 target. MicroRNAs and their targets can be co-expressed or expressed in a mutually exclusive fashion and the different roles and modes of microRNA action have been reviewed (Bushati and Cohen, 2007). We show here that both *EYA4* and miR-128 are co-expressed in the myotome, albeit at low levels (Fig. 1). This is consistent with the observation that miRNA targets are often expressed at very low levels, possibly at that of noise, in miRNA-expressing cells. It has been proposed that in such cases, the job of the miRNA is to keep low-level expression to inconsequential levels.

Luciferase assays also confirmed that miR-206 can negatively regulate the 3'UTR of *EYA4* and that miR-128 and miR-206 act together, with their combined effects being greater than their individual effects (Fig. 3E). *In vivo* experiments showed a similar trend. Quantitative RT-PCR of somites injected with either AM-128, AM-206, or both AM-128/AM-206 showed de-repression of *EYA4*. The effect after combined KD was greater than the sum of the separate effects of miR-128 or miR-206, suggesting cooperativity (Fig. 6E). Similar to miR-128, miR-206 is also expressed in the myotome and we showed previously that it regulates *PAX3*, thereby regulating the myogenic progenitor to committed myoblast transition (Goljanek-Whysall *et al.*, 2011). This raises the possibility that miR-128 and miR-206 also cooperate *in vivo* targeting multiple members of the PSED network, including *EYA4* and *PAX3*, via direct and indirect mechanisms.

Interestingly, the highly related microRNAs miR-27b and miR-1 did not affect expression of the *EYA4* 3'UTR luciferase reporter (Fig. 3F, G). The seed sequences of miR-27b and miR-128 overlap and the seeds of miR-1 and miR-206 are identical. Target recognition seems to be mediated mainly by the seed region, but there is a recognised contribution of 3' supplementary pairing between microRNAs and their targets, which might explain our findings.

To determine if other PSED members might be regulated by microRNAs known to be involved in myogenesis, we identified potential target sites for miR-128, miR-27b, miR-1, miR-206 and miR-133 in the 3'UTRs of *EYA1*, *EYA3*, *SIX1*, *SIX4* and *DACH1*. Luciferase reporters showed that *EYA1* has two target sites that can be recognised by miR-128 but not by the related miR-27b (Fig. 4A, F, G). *EYA1* and *EYA3* each have one target site for miR-

133 (Fig. 4A-D) and *SIX1* and *SIX4* each have one target site that is recognised by both miR-1 and miR-206 (Fig. 5A-D). Furthermore, *DACH1* has two sites recognised by both miR-1 and miR-206 and these seem to work independently of each other (Fig. 5A, B, E).

Overall our data suggest that fine-tuning levels of the PSED transcriptional regulators in developing somites by multiple microRNAs, miR-128, miR-1, miR-206 and miR-133, is important for the myogenic differentiation programme. In addition, we identify miR-128 as a novel microRNA required for myogenesis and *EYA4* as an important direct target. In particular, we propose that inhibiting the negative regulation of *Eya4* by miR-128 leads to elevated *EYA4* levels, which together with *Six4* activates expression of *Pax3*; preventing thus the entry into the differentiation programme, as indicated by loss of *MyoD1* expression (Fig. 6H). This model is supported by *PAX3* KD, which restores myogenesis in miR-128 KD somites (Fig. 6G).

Material and Methods

Culture and staging of embryos

Fertilised White Leghorn chicken eggs (Henry Stewart & Co Ltd, UK) were incubated at 38°C until they reached the desired stage of development according to (Hamburger and Hamilton, 1951).

Probes, *in situ* hybridisation, sections and photography

Fragments of chicken *EYA4* and *SIX4* coding sequences were PCR amplified from embryonic cDNA using primers for *Gga-EYA4* [NM_001305177.1] and *Gga-SIX4* [XM_003641442.2], cloned into pGEM-T Easy vector (Promega) and validated by sequencing. Antisense Digoxigenin-labelled RNA probes were generated for whole-mount *in situ* hybridisations as described (Mok *et al.*, 2018). Double-DIG-labelled LNA oligonucleotide-containing probes for miR-128 (Exiqon) were used as described (Ahmed *et al.*, 2015) (Suppl. Tables 1, 2). After colour reaction, embryos were de-stained in 5X TBST detergent mix and photographed on a Zeiss SV11 stereo-microscope using QCapture software. For cryosectioning, PFA-fixed embryos were embedded in O.C.T., 20 µm sections were collected on SuperFrost-Plus slides, mounted with Hydromount and photographed on a Zeiss AxioPlan microscope using AxioVision software.

DNA constructs, transfections and luciferase assay

Chicken *EYA1*, *EYA3*, *EYA4*, *SIX1*, *SIX4* and *DACH1* 3'UTR fragments containing predicted binding sites of miR-1a, miR-206 and miR-133a, miR-27b and miR-128 were PCR amplified and sub-cloned downstream of the luciferase gene as before (Goljanek-Whysall *et al.*, 2014). Mutant constructs were generated using FastCloning; miRNA target sites predicted by TargetScan and MiRanda algorithms (Betel *et al.*, 2008; Agarwal *et al.*, 2015)

were replaced with restriction enzyme sites introducing point mutations. All constructs were validated by sequencing (Suppl. Table 1, 3).

Chick dermal fibroblast (DF1) were seeded into 96-well plates at 7×10^4 cells/cm² and transfected in triplicate with Renilla and firefly luciferase reporter plasmids (25 ng, 100 ng) with miRNA mimics, identical to endogenous mature miRNAs, or si-control (siC) (50 nM, Sigma) using Lipofectamine 2000 (Invitrogen). After 24 hours luciferase activities were assayed in cell lysates using the Dual-Luciferase Reporter Assay System (Promega) and a multi-label counter (Promega GloMax). Relative luciferase activities were obtained by calculating the ratios of Firefly to Renilla luciferase activity, which was normalised to siC-treated samples.

Cloning of chicken *EYA4*, injection and electroporation into somites

The full-length coding region of chicken *EYA4* was PCR amplified from HH19-20 somite cDNA using SuperScript III Reverse Transcriptase kit (Invitrogen). Primer design used predicted *EYA4* sequences for chicken (ENSGALG00000031656) available from Ensembl Genome Browser (www.ensembl.org) (Suppl. Table 4). PCR products were subcloned into the pCA β expression vector and validated by sequencing.

Eggs were windowed and black ink was injected underneath the blastoderm to visualise the embryos. AntagomiRs AM-128, AM-206 and scrambled antagomiR (AM-scr) (Dharmacon) were designed as described (Goljanek-Whysall *et al.*, 2011) and injected into the posterior six somites of HH13-14 embryos, final concentration 1mM (Suppl. Table 5). After 24h embryos were harvested and processed for *in situ* hybridisation (Suppl. Fig. 1), or injected somites were dissected and processed for RNA extraction. Corresponding somites from the non-injected side were collected and used as control.

Expression construct (pCA β -*Gga-Eya4*, 2 mg/mL) was injected into the posterior six somites of HH13-14 embryos and electroporated using five 20 ms pulses of 50 V for 100 ms (Sweetman *et al.*, 2008). Plasmids produce GFP for tracing. Embryos were harvested after 24 h and those showing GFP fluorescence in targeted somites were processed.

PAX3 (*PAX3-MO*) and scrambled (*MO-scr*) morpholinos were 3' fluorescein (FITC)-labelled (Gene Tools; Suppl. Table 6). *PAX3-MO*, or *MO-scr*, was co-injected with AM-128 into the six most posterior somites of HH13-14 embryos, followed by electroporation using six 10-ms pulses of 60 V. Embryos were harvested after 24h.

RNA extraction and RT-qPCR

TRIzol reagent (Ambion) was used to isolate RNA from somites according to manufacturer's instructions; RNA was DNase treated (Roche) and extracted using acid phenol-chloroform (Ambion). cDNA was synthesised using random hexamer primers (Invitrogen) and SuperScript II Reverse Transcriptase kit (Invitrogen). RT-qPCRs were

performed in 96-well plates on ABI Prism 7500 (Applied Biosystems) using SYBR Green according to manufacturer's instructions. Primers (Sigma) were designed with PrimeTime (<https://eu.idtdna.com/scitools/Applications/RealTimePCR/>) (Suppl. Table 7). Relative quantifications were calculated using the Relative Standard Curve method (Larionov, Krause and Miller, 2005) and normalised to the averaged relative quantification of β -actin and GAPDH housekeeping genes. Results from injected somites were compared to their contralateral non-injected somites, expressed in \log_{10} (fold change) and plotted on a linear scale where the x-axis corresponds to the non-injected condition set at 0 ($\log_{10}(1)=0$).

Computational methods

MiRNA sequences were collected from XenmiR, GEISHA and miRBase databases (Kozomara and Griffiths-Jones, 2014; Ahmed *et al.*, 2015). Potential miRNA targets were identified using TargetScan (Lewis, Burge and Bartel, 2005; Agarwal *et al.*, 2015). Identification of potential miRNAs targeting mRNAs of interest was done using miRanda (John *et al.*, 2004; Betel *et al.*, 2008). GO term analysis was assessed using DAVID bioinformatics resources and g:Profiler (Reimand *et al.*, 2007, 2016; Huang, Lempicki and Sherman, 2009; Huang, Sherman and Lempicki, 2009). A MiRanda, GO term and KEGG pathway annotation analysis was performed for all the miRNAs presented in Suppl. Table 1, except miR-128 investigated in this work, using DAVID tool (Release 7.2; March 2018) (Suppl. Table 8). For each miRNA, the number of predicted targets is indicated. Genes from categories of interest have been listed. Genes from the PSED network have been underlined.

Statistical analysis

Luciferase assays and RT-qPCR data were analysed with GraphPad Prism 8 using Student's two-tailed unpaired *t*-test and Mann Whitney *U*-test to assess the differences in one variable between non-treated and treated samples. The data are presented as the means \pm S.E.M. unless indicated and are representative of at least three independent experiments. In all statistical analysis, $p < 0.05$ was considered significant.

Acknowledgements

We thank Timothy Grocott for help with cloning and luciferase assays and for discussions, Gi Fay Mok for help with microinjection and electroporation, Tracey Swingler for help with qPCR, Simon Moxon for help with bioinformatics. CV and SM were funded by the BBSRC Doctoral Training Programme on the Norwich Research Park (NRPDTP). Research was supported by BBSRC project grants to AM (BB/K003437, BB/N007034).

References

- Abu-Elmagd, M. *et al.* (2015) 'Sprouty2 mediated tuning of signaling is essential for somite myogenesis.', *BMC medical genomics*. BioMed Central Ltd, 8 Suppl 1(1), p. S8. doi: 10.1186/1755-8794-8-S1-S8.
- Agarwal, V. *et al.* (2015) 'Predicting effective microRNA target sites in mammalian mRNAs', *eLife*, 4(AUGUST2015), pp. 1–38. doi: 10.7554/eLife.05005.
- Ahmed, A. *et al.* (2015) 'A database of microRNA expression patterns in *Xenopus laevis*', *PLoS ONE*, 10(10), pp. 1–10. doi: 10.1371/journal.pone.0138313.
- Bajard, L. *et al.* (2006) 'A novel genetic hierarchy functions during hypaxial myogenesis: Pax3 directly activates Myf5 in muscle progenitor cells in the limb', *Genes and Development*, 20(17), pp. 2450–2464. doi: 10.1101/gad.382806.
- Bartel, D. P. (2004) 'MicroRNAs: Genomics, Biogenesis, Mechanism, and Function', *Cell*, 116(2), pp. 281–297. doi: 10.1016/S0092-8674(04)00045-5.
- Bartel, D. P. (2009) 'MicroRNAs: Target Recognition and Regulatory Functions', *Cell*, 136(2), pp. 215–233. doi: 10.1016/j.cell.2009.01.002.
- Bartel, D. P. (2018) 'Metazoan MicroRNAs', *Cell*, 173(1), pp. 20-51. doi: 10.1016/j.cell.2018.03.006
- Berkes, C. A. and Tapscott, S. J. (2005) 'MyoD and the transcriptional control of myogenesis', *Seminars in Cell and Developmental Biology*, 16(4–5), pp. 585–595. doi: 10.1016/j.semcdb.2005.07.006.
- Betel, D. *et al.* (2008) 'The microRNA.org resource: Targets and expression', *Nucleic Acids Research*, 36(SUPPL. 1), pp. 149–153. doi: 10.1093/nar/gkm995.
- Bober, E. *et al.* (1994) 'Pax-3 is required for the development of limb muscles: a possible role for the migration of dermomyotomal muscle progenitor cells.', *Development*, 120(3), pp. 603–612.
- Brent, A. E. and Tabin, C. J. (2002) 'Developmental regulation of somite derivatives: Muscle, cartilage and tendon', *Current Opinion in Genetics and Development*, 12(5), pp. 548–557. doi: 10.1016/S0959-437X(02)00339-8.
- Bruno, I. G. *et al.* (2011) 'Identification of a MicroRNA that Activates Gene Expression by Repressing Nonsense-Mediated RNA Decay', *Molecular Cell*, 42(4), pp. 500–510. doi: 10.1016/j.molcel.2011.04.018.Identification.
- Buckingham, M. and Relaix, F. (2007) 'The role of Pax genes in the development of tissues and organs: Pax3 and Pax7 regulate muscle progenitor cell functions.', *Annual review of cell and developmental biology*, 23, pp. 645–73. doi: 10.1146/annurev.cellbio.23.090506.123438.
- Buckingham, M. and Rigby, P. W. J. (2014) 'Gene Regulatory Networks and Transcriptional Mechanisms that Control Myogenesis', *Developmental Cell*. Elsevier Inc., 28(3), pp. 225–238. doi: 10.1016/j.devcel.2013.12.020.
- Bushati and Cohen (2007) 'microRNA Functions', *Annu. Rev. Cell Dev. Biol.* 23, pp. 175-205. doi: 10.1146/annurev.cellbio.23.090506.123406
- Christ, B., Huang, R. and Scaal, M. (2007) 'Amniote somite derivatives', *Developmental Dynamics*, 236(9), pp. 2382–2396. doi: 10.1002/dvdy.21189.
- Christ, B. and Ordahl, C. P. (1995) 'Early stages of chick somite development', *Anatomy and Embryology*, 191(5), pp. 381–396. doi: 10.1007/BF00304424.
- Darnell, D. K. *et al.* (2006) 'MicroRNA expression during chick embryo development', *Developmental Dynamics*, 235(11), pp. 3156–3165. doi: 10.1002/dvdy.20956.
- Ekimler, S. and Sahin, K. (2014) 'Computational Methods for MicroRNA Target Prediction', *Genes*, 5(3), pp. 671–683. doi: 10.3390/genes5030671.
- Giordani, J. *et al.* (2007) 'Six proteins regulate the activation of Myf5 expression in embryonic mouse limbs', *Proceedings of the National Academy of Sciences*, 104(27), pp. 11310–11315. doi: 10.1073/pnas.0611299104.
- Goljanek-Whysall, K. *et al.* (2011) 'MicroRNA regulation of the paired-box transcription factor Pax3 confers robustness to developmental timing of myogenesis.', *Proceedings of the National Academy of Sciences of the United States of America*, 108(29), pp. 11936–41. doi: 10.1073/pnas.1105362108.
- Goljanek-Whysall, K. *et al.* (2014) 'myomiR-dependent switching of BAF60 variant incorporation into Brg1 chromatin remodeling complexes during embryo myogenesis', *Development*, 141(17), pp. 3378–3387. doi: 10.1242/dev.108787.
- Goulding, M., Lumsden, A. and Paquette, A. J. (1994) 'Regulation of Pax-3 expression in the

- dermomyotome and its role in muscle development.', *Development*, 120(4), pp. 557–571.
- Grifone, R. *et al.* (2005) 'Six1 and Six4 homeoproteins are required for Pax3 and Mrf expression during myogenesis in the mouse embryo.', *Development*, 132(9), pp. 2235–49. doi: 10.1242/dev.01773.
- Grifone, R. *et al.* (2007) 'Eya1 and Eya2 proteins are required for hypaxial somitic myogenesis in the mouse embryo', *Developmental Biology*, 302, pp. 602–616. doi: 10.1016/j.ydbio.2006.08.059.
- Gros, J., Scaal, M. and Marcelle, C. (2004) 'A two-Step mechanism for myotome formation in chick', *Developmental Cell*, 6(6), pp. 875–882. doi: 10.1016/j.devcel.2004.05.006.
- Hamburger, V. and Hamilton, H. L. (1951) 'A series of normal stages in the development of the chick embryo', *Journal of Morphology*, 88(1), pp. 49–92. doi: doi:10.1002/jmor.1050880104.
- Hancock, J. M. *et al.* (2004) 'EMBOSS (The European Molecular Biology Open Software Suite)', in *Dictionary of Bioinformatics and Computational Biology*. John Wiley & Sons, Ltd. doi: 10.1002/9780471650126.dob0206.pub2.
- Heanue, T. A. *et al.* (1999) 'Synergistic regulation of vertebrate muscle development by Dach2, Eya2, and Six1, homologs of genes required for Drosophila eye formation', *Genes and Development*, 13(24), pp. 3231–3243. doi: 10.1101/gad.13.24.3231.
- Huang, D. W., Lempicki, R. a and Sherman, B. T. (2009) 'Systematic and integrative analysis of large gene lists using DAVID bioinformatics resources.', *Nature Protocols*, 4(1), pp. 44–57. doi: 10.1038/nprot.2008.211.
- Huang, D. W., Sherman, B. T. and Lempicki, R. A. (2009) 'Bioinformatics enrichment tools: Paths toward the comprehensive functional analysis of large gene lists', *Nucleic Acids Research*, 37(1), pp. 1–13. doi: 10.1093/nar/gkn923.
- Ivanovska, I. and Cleary, M. A. (2008) 'Combinatorial microRNAs: Working together to make a difference', *Cell Cycle*, 7(20), pp. 3137–3142. doi: 10.4161/cc.7.20.6923.
- Jemc, J. and Rebay, I. (2007) 'The eyes absent family of phosphotyrosine phosphatases: properties and roles in developmental regulation of transcription.', *Annual review of biochemistry*, 76, pp. 513–538. doi: 10.1146/annurev.biochem.76.052705.164916.
- John, B. *et al.* (2004) 'Human MicroRNA targets.', *PLoS biology*, 2(11), p. e363. doi: 10.1371/journal.pbio.0020363.
- Kapsimali, M. *et al.* (2007) 'MicroRNAs show a wide diversity of expression profiles in the developing and mature central nervous system.', *Genome biology*, 8(8), p. R173. doi: 10.1186/gb-2007-8-8-r173.
- Kassar-Duchossoy, L. *et al.* (2005) 'Pax3/Pax7 mark a novel population of primitive myogenic cells during development', *Genes and Development*, 19(12), pp. 1426–1431. doi: 10.1101/gad.345505.
- Kozomara, A. and Griffiths-Jones, S. (2014) 'MiRBase: Annotating high confidence microRNAs using deep sequencing data', *Nucleic Acids Research*, 42(D1), pp. 68–73. doi: 10.1093/nar/gkt1181.
- Kumar, J. (2009) 'The sine oculis homeobox (SIX) family of transcription factors as regulators of development and disease', *Cell Mol Life Sci.*, 66(4), pp. 565–583. doi: 10.1007/s00018-008-8335-4.The.
- Laclef, C. *et al.* (2003) 'Altered myogenesis in Six1-deficient mice.', *Development*, 130(10), pp. 2239–2252. doi: 10.1242/dev.00440.
- Lagos-Quintana, M. *et al.* (2002) 'Identification of tissue-specific MicroRNAs from mouse', *Current Biology*, 12(9), pp. 735–739. doi: 10.1016/S0960-9822(02)00809-6.
- Larionov, A., Krause, A. and Miller, W. (2005) 'A standard curve based method for relative real time PCR data processing', *BMC bioinformatics*, 6, p. 62. doi: 10.1186/1471-2105-6-62.
- Lewis, B. P., Burge, C. B. and Bartel, D. P. (2005) 'Conserved seed pairing, often flanked by adenosines, indicates that thousands of human genes are microRNA targets', *Cell*, 120(1), pp. 15–20. doi: 10.1016/j.cell.2004.12.035.
- Li, W. *et al.* (2015) 'The EMBL-EBI bioinformatics web and programmatic tools framework.', *Nucleic acids research*, 43(W1), pp. W580-4. doi: 10.1093/nar/gkv279.
- Li, X. *et al.* (2003) 'Eya protein phosphatase activity regulates Six1-Dach-Eya transcriptional effects in mammalian organogenesis.', *Nature*, 426(6964), pp. 247–254. doi: 10.1038/nature02283.

- Lin, S. *et al.* (2012) 'Let-7b regulates the expression of the growth hormone receptor gene in deletion-type dwarf chickens.', *BMC genomics*. BMC Genomics, 13(1), p. 306. doi: 10.1186/1471-2164-13-306.
- Long, D. *et al.* (2007) 'Potent effect of target structure on microRNA function.', *Nature structural & molecular biology*, 14(APRIL), pp. 287–294. doi: 10.1038/nsmb1226.
- Lu, J. and Clark, A. G. (2012) 'Impact of microRNA regulation on variation in human gene expression', *Genome Research*, 22, pp. 1243–1254. doi: 10.1101/gr.132514.111.22.
- Mansouri, A. *et al.* (1996) 'Dysgenesis of cephalic neural crest derivatives in Pax7^{-/-} mutant mice.', *Development*, 122(3), pp. 831–8.
- Maroto, M. *et al.* (1997) 'Ectopic Pax-3 activates MyoD and Myf-5 expression in embryonic mesoderm and neural tissue.', *Cell*, 89(1), pp. 139–148. doi: 10.1016/S0092-8674(00)80190-7.
- Mok, G. F. *et al.* (2018) 'Mir-133-mediated regulation of the hedgehog pathway orchestrates embryo myogenesis', *Development (Cambridge)*, 145(12). doi: 10.1242/dev.159657.
- Mok, G. F. *et al.* (2020) 'Characterising open chromatin identifies novel cis-regulatory elements important for paraxial mesoderm formation and axis extension', *BioRxiv*. doi: 10.1017/CBO9781107415324.004.
- Mok, G. F., Lozano-Velasco, E. and Münsterberg, A. (2017) 'microRNAs in skeletal muscle development', *Seminars in Cell and Developmental Biology*. Elsevier Ltd, 72, pp. 67–76. doi: 10.1016/j.semcd.2017.10.032.
- Motohashi, N. *et al.* (2013) 'Regulation of IRS1/Akt insulin signaling by microRNA-128a during myogenesis.', *Journal of Cell Science*, 126, pp. 2678–2691. doi: 10.1242/jcs.119966.
- Ohto, H. *et al.* (1999) 'Cooperation of Six and Eya in Activation of Their Target Genes through Nuclear Translocation of Eya', *Molecular and cellular biology*, 19(10), pp. 6815–6824.
- Ozaki, H. *et al.* (2001) 'Six4, a putative myogenin gene regulator, is not essential for mouse embryonal development.', *Molecular and cellular biology*, 21(10), pp. 3343–50. doi: 10.1128/MCB.21.10.3343-3350.2001.
- Ozaki, H. *et al.* (2004) 'Six1 controls patterning of the mouse otic vesicle.', *Development (Cambr)*, 131(3), pp. 551–562. doi: 10.1242/dev.00943.
- Rayapureddi, J. P. *et al.* (2003) 'Eyes absent represents a class of protein tyrosine phosphatases.', *Nature*, 426(6964), pp. 295–8. doi: 10.1038/nature02093.
- Reimand, J. *et al.* (2007) 'G:Profiler—a web-based toolset for functional profiling of gene lists from large-scale experiments', *Nucleic Acids Research*, 35(SUPPL.2), pp. 193–200. doi: 10.1093/nar/gkm226.
- Reimand, J. *et al.* (2016) 'g:Profiler—a web server for functional interpretation of gene lists (2016 update)', *Nucleic Acids Research*, pp. 1–7. doi: 10.1093/nar/gkw199.
- Relaix, F. *et al.* (2005) 'A Pax3/Pax7-dependent population of skeletal muscle progenitor cells.', *Nature*, 435(7044), pp. 948–53. doi: 10.1038/nature03594.
- Relaix, F. *et al.* (2013) 'Six Homeoproteins Directly Activate Myod Expression in the Gene Regulatory Networks That Control Early Myogenesis', *PLoS Genetics*, 9(4). doi: 10.1371/journal.pgen.1003425.
- Relaix, F. and Buckingham, M. (1999) 'From insect eye to vertebrate muscle: redeployment of a regulatory network', *Genes and Development*, pp. 3171–3178.
- Selbach, M. *et al.* (2008) 'Widespread changes in protein synthesis induced by microRNAs', *Nature*, 455(7209), pp. 58–63. doi: 10.1038/nature07228.
- Sempere, L. F. *et al.* (2004) 'Expression profiling of mammalian microRNAs uncovers a subset of brain-expressed microRNAs with possible roles in murine and human neuronal differentiation.', *Genome biology*, 5(3), p. R13. doi: 10.1186/gb-2004-5-3-r13.
- Shi, L. *et al.* (2015) 'MicroRNA-128 targets myostatin at coding domain sequence to regulate myoblasts in skeletal muscle development', *Cellular Signalling*. Elsevier Inc., 27(9), pp. 1895–1904. doi: 10.1016/j.cellsig.2015.05.001.
- Spitz, F. *et al.* (1998) 'Expression of myogenin during embryogenesis is controlled by Six/sine oculis homeoproteins through a conserved MEF3 binding site', *Proc Natl Acad Sci U S A*, 95, pp. 14220–14225. doi: 10.1073/pnas.95.24.14220.
- Sweetman, D. *et al.* (2006) 'FGF-4 signaling is involved in mir-206 expression in developing somites of chicken embryos', *Developmental Dynamics*, 235(8), pp. 2185–2191. doi:

10.1002/dvdy.20001.

Sweetman, D. *et al.* (2008) 'Specific requirements of MRFs for the expression of muscle specific microRNAs, miR-1, miR-206 and miR-133', *Developmental Biology*, 321(2), pp. 491–499. doi: 10.1016/j.ydbio.2008.06.019.

Tajbakhsh, S. *et al.* (1997) 'Redefining the genetic hierarchies controlling skeletal myogenesis: Pax-3 and Myf-5 act upstream of MyoD.', *Cell*, 89(1), pp. 127–138. doi: 10.1016/S0092-8674(00)80189-0.

Tapscott, S. J. (2005) 'The circuitry of a master switch: Myod and the regulation of skeletal muscle gene transcription', *Development*, 132(12), pp. 2685–2695. doi: 10.1242/dev.01874.

Tootle, T. L. *et al.* (2003) 'The transcription factor Eyes absent is a protein tyrosine phosphatase', *Nature*, 426, pp. 299–302. doi: 10.1038/nature02097.

Williams, B. a and Ordahl, C. P. (1994) 'Pax-3 expression in segmental mesoderm marks early stages in myogenic cell specification.', *Development*, 120(4), pp. 785–796.

Witman, N. *et al.* (2013) 'MiR-128 regulates non-myocyte hyperplasia, deposition of extracellular matrix and Islet1 expression during newt cardiac regeneration', *Developmental Biology*. Elsevier, 383(2), pp. 253–263. doi: 10.1016/j.ydbio.2013.09.011.

Xu, H. *et al.* (2006) 'Identification of microRNAs from different tissues of chicken embryo and adult chicken', *FEBS Letters*, 580(15), pp. 3610–3616. doi: 10.1016/j.febslet.2006.05.044.

Yusuf, F. and Brand-Saberi, B. (2006) 'The eventful somite: Patterning, fate determination and cell division in the somite', *Anatomy and Embryology*, 211(SUPPL. 1), pp. 21–30. doi: 10.1007/s00429-006-0119-8.

Zhou, B. *et al.* (2010) 'MicroRNA expression profiles of porcine skeletal muscle', *Animal Genetics*, 41(5), pp. 499–508. doi: 10.1111/j.1365-2052.2010.02026.x.

Figure Legends

Fig. 1: MiR-128 and *EYA4* are both expressed in the myotome. Expression profiles of miR-1a (A), miR-206 (B) and miR-133a (C) at different stages. Expression profiles of miR-128 (D) and *EYA4* (E) were determined by whole-mount *in situ* hybridisation at different stages. The level of transverse sections at HH11-12 (i-i')(iv-iv'), HH16 (ii-ii')(v-v'), and HH21-22 (iii-iii')(vi-vi') are indicated by a red line. (D) At HH11-12, miR-128 is expressed in the neural tube (NT) and the developing somites (i'). At HH16 and HH21-22, miR-128 is in the branchial arches, in the myotome, and the developing limbs (ii-iii'). At HH21-22, miR-128 is also expressed around the eye, and in the limbs (iii; white asterisk). (E) WMISH performed with antisense DIG-labelled RNA probe, and transverse sections at HH11-12, HH16, and HH21-22 At HH11-12 (iv-iv'). *EYA4* is expressed in the eye (e), the otic vesicle (vOt), and in a pool of non-identified migrating cells close to the heart region (iv; asterisk). At HH16 (v-v'), *EYA4* is expressed in the eye, the branchial arches (v; arrow) and in the somites (s), in the myotome (v'; My). At HH21-22 (vi-vi'). *EYA4* is still expressed in the branchial arches (vi; arrow), and is strongly expressed in the myotome (vi'). *EYA4* is also found dorsally in the posterior limb buds (vi; arrowhead). No expression was detected on embryos treated with the sense probe (negative control; data not shown). E: eye; My: myotome; NC: notochord; NT: neural tube; S: somite; vOt: otic vesicle.

Fig. 2: Many predicted miR-128 target genes are involved in developmental processes. (A) Gene Ontology analysis of miR-128 muscle targets predicted by TargetScan. (B) Venn diagramme of the genes included in the category "Developmental process" using either GO term or g:GOST. (C) For the 126 genes identified by both analyses the UP_TISSUE terms are shown. (D) The miR-128 muscle-enriched target genes (10) include *EYA4*. (E) Percentage ID and SIM between predicted Gga-*EYA4* and human (Hsa) [NP_004091.3], mouse (Mmu) [NP_034297.2], and *Xenopus tropicalis* (Xtr) [ENSXETT00000000214.3]. (F) Percentage identity (ID) and similarity (SIM) between predicted Gga-*EYA4* [ENSGALT00000022662.4] and the three other chicken EYA members, predicted Gga-*EYA1* [XP_418290.3], Gga-*EYA2* [NP_990246.1], and predicted Gga-*EYA3* [XP_417715.2]. Percentage ID and SIM were determined using EMBOSS Needle software (http://www.ebi.ac.uk/Tools/psa/emboss_needle/) (Hancock *et al.*, 2004; Li *et al.*, 2015).

Fig. 3: The *EYA4* 3'UTR contains functional target sites for miR-128 and miR-206. (A) Schematic of *EYA4* transcript with coding region (box) and 3'UTR (dotted line). Red and green arrows indicate the position of primer pairs used to clone the fragments of coding and 3'UTR sequences which were used for ISH and luciferase reporter assays, respectively. The positions of putative miR-1a/206, miR-27b/128 and miR-133 binding sites are indicated. (B) Alignment of miR-128 and miR-27b shows that the seed sequences are conserved but they have poor homology outside the seed. Alignment of miR-1a with miR-206 shows that they

are very similar. Alignments of each of these microRNAs with their predicted target sites in the *EYA4* 3'UTR. Mutations introduced into the predicted target sites were designed to disrupt base pairing in the seed region (mutated nucleotides are indicated in red). Vertical lines indicate complementarity and asterisks indicate identity between sequences. **(C-G)** Relative luciferase activity for Gga-*EYA4* 3'UTR reporter assays is shown, wild-type (WT) or mutants were co-transfected either with control siRNA (siC; white columns), or with mimics for miR-128 **(C)**, miR-206 **(D)**, miR-128 and miR-206 **(E)**, miR-27b **(F)**, or miR-1a **(G)** (black, grey shaded columns). Normalised luciferase activity was plotted relative to the siC condition. Experiments were repeated at least four times independently with triplicate samples in each. Error bars represent the standard error of the mean (SEM). Unpaired *t*-test: $p < 0.01$: **, $p < 0.001$: ***.

Fig. 4: The *EYA1* and *EYA3* 3'UTRs contain functional target sites for miR-133a. **(A)** Schematic of *EYA1* and *EYA3* transcripts with coding region (box) and 3'UTR (dotted line). Green arrows indicate the position of primer pairs used to clone the fragments of 3'UTR sequences which were used for luciferase reporter assays. The positions of putative miR-27b/128 and miR-133 binding sites are indicated. **(B)** Alignments of *EYA1*, *EYA3* and *EYA4* 3'UTR predicted target sequences with miR-133a; mutated nucleotides disrupting seed-pairing in red. **(C-E)** Relative luciferase activity for Gga-*EYA1*, or Gga-*EYA3*, or Gga-*EYA4* 3'UTR reporter assays is shown, wild-type (WT) or mutants were co-transfected either with control siRNA (siC; white columns), or with mimics for miR-133a (black columns). **(F)** Alignments of Gga-*EYA1* 3'UTR predicted miR-27b/miR-128 target sequences with miR-27b and miR-128 sequences. **(G)** Relative luciferase activity for Gga-*EYA1* 3'UTR construct, wild-type (WT) and mutants (single and double mutants), co-transfected either with control siRNA (siC; white), or with mimics for miR-27b (black), or miR-128 (grey). Experiments were repeated 3 times independently with triplicate samples in each. Error bars represent the standard error of the mean (SEM). Unpaired *t*-test: $p < 0.001$: ***.

Fig. 5: The PSED members *SIX1*, *SIX4* and *DACH1* are regulated by miR-1a/miR-206. **(A)** Schematic of *SIX1*, *SIX4* and *DACH1* transcripts with coding region (box) and 3'UTR (dotted line). Green arrows indicate the position of primer pairs used to clone 3'UTR fragments used for luciferase reporter assays. The positions of putative miR-1a/miR-206 and miR-133 binding sites are indicated. Red arrows indicate the position of primer pairs used to clone a *SIX4* fragment used for ISH. **(B)** Alignments of *SIX1*, *SIX4* and *DACH1* 3'UTR predicted target sequences with miR-1a and miR-206; mutated nucleotides disrupting seed-pairing in red. **(C-E)** Relative luciferase activity for Gga-*SIX1* **(C)**, Gga-*SIX4* **(D)** and Gga-*DACH1* **(E)** 3'UTR constructs, wild-type (WT) and mutants, co-transfected either with control siRNA (siC; white), or with mimics for miR-1a (black) or miR-206 (grey). Experiments were

repeated at least 3 times independently with triplicate samples in each. Error bars represent the standard error of the mean (SEM). Unpaired *t*-test: $p < 0.05$: *; $p < 0.01$: **; $p < 0.001$: ***.

Fig. 6: MiR-128 regulates myogenesis through its interaction with *EYA4*. AntagomiR-128 (1 mM) was injected into the 6 most posterior somites, on one side of HH13-14 embryos. After 24h incubation, HH19-20 embryos were processed for ISH to detect the transcripts indicated. To identify injected somites the FITC-coupled antagomiR-128 or antagomiR-scr was detected using Fast Red. **(A)** Expression patterns in whole-mount embryos, dorsal view. **(B)** Transverse sections (red dotted lines) at the interlimb level showing *EYA4*, *SIX4*, *PAX3* and *MYOD1* expression as indicated; Alexa-Fluor-568 reveals antagomiR location. The contralateral non-injected side (left side), was used as control. **(C)** Quantification of phenotypes observed. **(D)** PSED members and MRFs (*MYOD1*) transcript levels in somites injected with AM-128. RT-qPCR results expressed in \log_{10} (fold change). For each gene and each experiment, the injected somite data were normalised to two housekeeping genes (*GAPDH*+ β -actin) and compared to the contralateral non-injected somite data of the same embryo. Number of independent experiments for each tested gene after AM-128 injection: *DACH1* (n=6); *EYA4*, *SIX4*, *PAX3*, *MYOD1* (n=7); *EYA3*, *SIX1* (n=8); *EYA1*, *EYA2* (n=10). **(E)** *EYA4* and *PAX3* transcript levels in somites co-injected with AM-128 and AM-206. RT-qPCR results expressed in \log_{10} (fold change). **(F)** For targeted mis-expression *EYA4* expression construct was injected and electroporated into the 6 most posterior somites, on one side of HH13-14 embryos. After 24h incubation, HH19-20 embryos were collected, injected somites were dissected for RNA extraction. RT-qPCR showed the deregulation of PSED members (*EYA4*, *SIX4*, *PAX3*) and *MYOD1* transcripts as (\log_{10} (fold change)) in electroporated somites compared to controls. At least seven independent experiments were performed for each gene. Mann-Whitney *U*-test: $p < 0.05$: *, $p < 0.001$: ***. **(G)** *In situ* hybridisation performed on embryos co-injected and electroporated with FITC-labelled *PAX3-MO* (ii-ii'') or scrambled morpholino (*MO-scr*) (i-i'') and AM-128 into the 6 most posterior somites, on one side of HH13-14 embryos. *MYOD1* expression is rescued in somites that received *PAX3-MO* and AM-128 (ii, ii') while in somites co-injected with *MO-scr* and AM-128, *MYOD1* expression loss is still observed (i, i'). Number of embryos analysed: *PAX3-MO*+AM-128 (n=8); *MO-scr*+AM-128 (n=6). **(H)** Summary: Inhibiting the negative regulation of *EYA4* by miR-128 led to de-repression of *EYA4*, which together with *SIX4* activates expression of *PAX3*. This prevents entry of myogenic progenitors into the differentiation programme, indicated by loss of *MYOD1* expression.

Table Legend

Table 1 MiRanda analysis. Each miRNA was used to scan the 3'UTR sequences of chicken (*Gallus gallus*, Gga) *EYA1* [ENSGALT000000025181.4], *EYA2* [ENSGALT00000007180.4], *EYA3* [ENSGALT00000001127.4], *EYA4* [ENSGALT00000022662.4], *SIX1* [NM_001044685.1], predicted *SIX4* [XM_003641442.2], and *DACH1* [ENSGALT00000027373.3]. #: MRE annotated in human sequence (TargetScan 'human'), and conserved in chicken (TargetScan 'chicken'). Predicted and validated targets are indicated in bold. nd: not studied in this work.

Journal Pre-proof

Suppl. Figure Legend

Suppl. Fig. 1 AntagomiR experiment. Localisation of the antagomiRs just after injection (i-iii'; T0) and 24h later (iv-vii'; T24h). AntagomiRs were injected in the 6 most posterior somites of HH13-14 embryos (i). After 24h, HH19-20 embryos were collected for further analyses. AntagomiRs are FITC-labelled allowing to visualise them before PFA-fixation (iii, iii'; iii', vi'). After fixation and WMISH, antagomiRs were detected using an alkaline phosphatase coupled anti-FITC antibody and revealed by Fast Red (vii, vii'); example of an HH19-20 embryo showing *MYOD1* expression (in blue) after AM-128 injection (in red). Details of the antagomiRs localisation (iii', vi', vii'; red-dotted square in iii, vi and vii). Red arrows indicate injected somites.

Journal Pre-proof

Suppl. Table Legend

Suppl. Table 1 MiRNA sequences used to run the miRanda algorithm.

Suppl. Table 2 (A) Probe sequences and **(B)** *in vitro* transcription conditions.

Suppl. Table 3 (A) Primers used to clone *EYA*, *SIX* and *DACH* 3'UTR fragments and **(B)** primers used to introduce mutations into miRNA sites. **(A)** For sub-cloning purpose, enzymatic restriction sites (underlined bases) were added to the 5'-end of the primers: BglII (AGATCT), NheI (GCTAGC). **(B)** Bases constituting miRNA sites are underlined and mutated nucleotides are indicated in red.

Suppl. Table 4 Primers used to clone full-length *Gga-EYA4*. For sub-cloning purpose, enzymatic restriction sites (underlined bases) were added to the 5'-end of the primers: NotI (GCGGCCGC), EcoRI (GAATTC). Start and stop codons are indicated in red. A HA-tag was added and is indicated in italic.

Suppl. Table 5 AntagomiR sequences. All bases were replaced by 2'O-methyl-bases, and some phosphodiester bonds were replaced by thiol bonds, indicated in the sequences by 'm' and '**', respectively. The antagomiRs were FITC-labelled at their 5'-end (F1), and included a 3' cholesterol moiety at their 3'-end (Ch1).

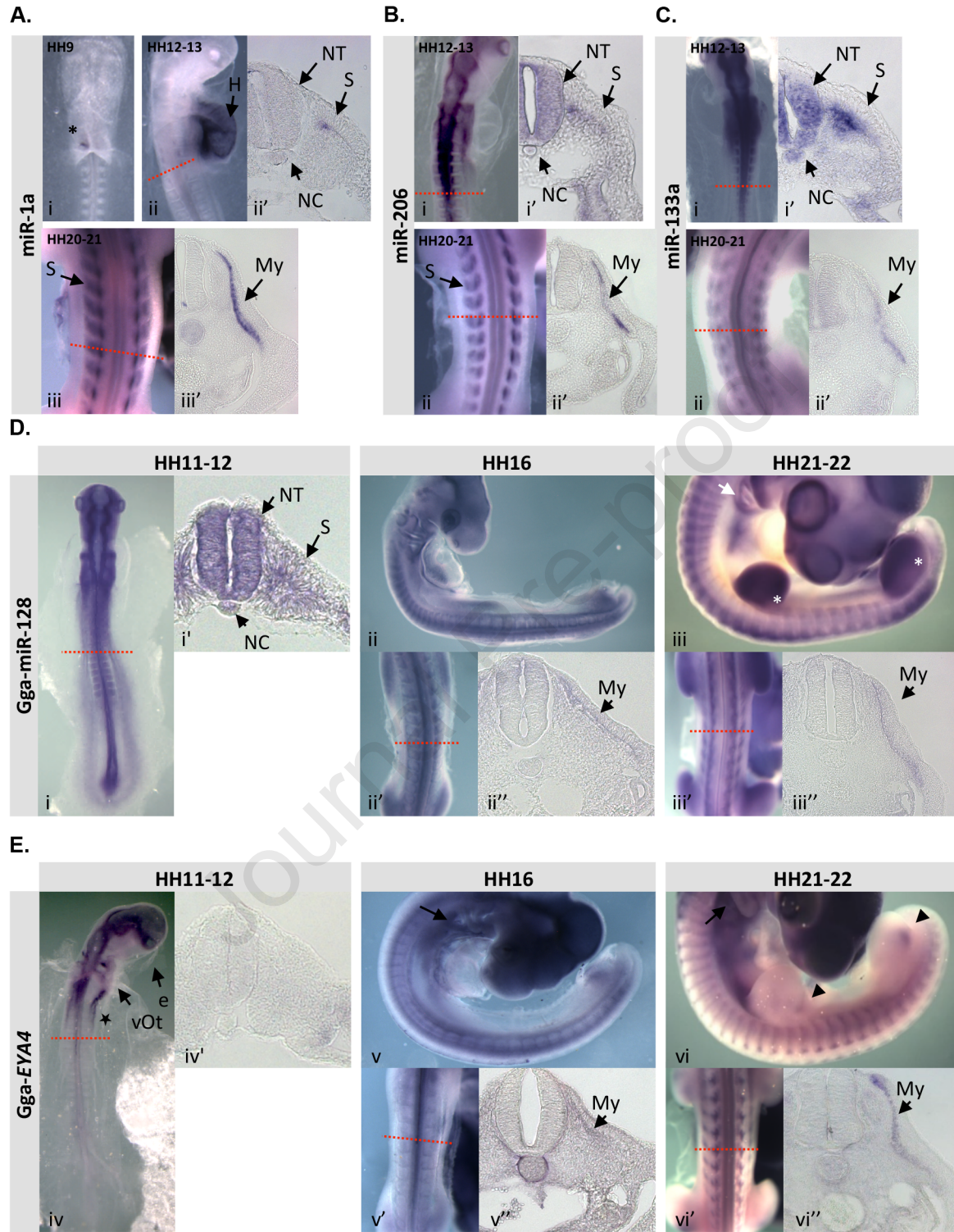
Suppl. Table 6 Morpholino sequences. The morpholinos were FITC-labelled at their 3'-end.

Suppl. Table 7 Quantitative PCR primer sequences.

Suppl. Table 8 MiRanda analysis. GO term and KEGG pathway annotation analysis performed using DAVID tool (Release 7.2 ; March 2018). For each miRNA, the number of predicted targets is indicated. Genes from categories of interest have been listed. Genes from the PSEN network have been underlined.

MiRNA	3'UTR						
	<i>EYA1</i>	<i>EYA2</i>	<i>EYA3</i>	<i>EYA4</i>	<i>SIX1</i>	<i>SIX4</i>	<i>DACH1</i>
Gga-miR-1a	X	X nd	X nd	X [#]	X	X	X
Gga-miR-27b-3p	X [#]	X nd	X nd	X [#]	X nd	X nd	X nd
Gga-miR-128	X	X nd		X[#]		X nd	
Gga-miR-133a		X nd	X	X [#]		X nd	X nd
Gga-miR-206			X nd	X[#]	X	X	X

Table 1 MiRanda analysis. Each miRNA was used to scan the 3'UTR sequences of chicken (*Gallus gallus*, Gga) *EYA1* [ENSGALT000000025181.4], *EYA2* [ENSGALT00000007180.4], *EYA3* [ENSGALT00000001127.4], *EYA4* [ENSGALT000000022662.4], *SIX1* [NM_001044685.1], predicted *SIX4* [XM_003641442.2], and *DACH1* [ENSGALT000000027373.3]. #: MRE annotated in human sequence (TargetScan 'human'), and conserved in chicken (TargetScan 'chicken'). Predicted and validated targets are indicated in bold. nd: not studied in this work.



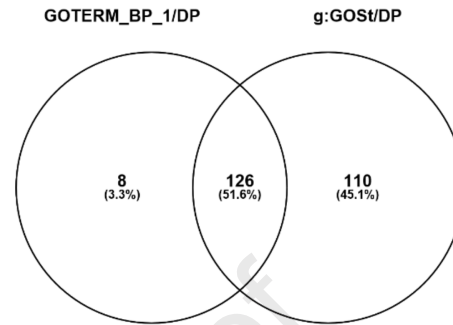
A.

Gene Ontology term

GOTERM_BP_1	Count	%	p-value
Cellular process	322	69.2	2.5E-6
Biological regulation	257	55.3	7.2E-9
Metabolic process	234	50.3	2.9E-3
Multicellular organismal process	144	31.0	1.3E-3
Developmental process	134	28.8	7.9E-9
Cellular component organisation	97	20.9	1.2E-4
Cellular component biogenesis	37	8.0	4.8E-2
Locomotion	21	4.5	1.3E-2
Growth	10	2.2	6.0E-2

g:GOST	Count	%	p-value
Biological regulation	357	73.9	2.0E-9
Regulation of biological process	349	72.3	1.4E-10
Regulation of cellular process	335	69.4	3.7E-10
Regulation of metabolic process	256	53.0	7.9E-14
Developmental process	236	48.9	3.6E-15
Positive regulation of biological process	206	42.7	6.4E-9
Gene expression	198	41.0	2.8E-7
Regulation of gene expression	187	38.7	6.3E-14
Regulation of developmental process	109	22.6	4.4E-10
Tissue development	83	17.2	1.2E-5

B.



C.

Enriched Gene Ontology term

UP_TISSUE	Count	%	p-value
Brain	65	51.6	2.0E-2
Placenta	31	24.6	4.1E-2
Epithelium	28	22.2	1.1E-2
Foetal brain	12	9.5	1.4E-2
Eye	12	9.5	7.6E-2
Amygdala	11	8.7	7.5E-3
Muscle	10	7.9	8.9E-2
Frontal cortex	3	2.4	1.5E-2
Foetal lung	3	2.4	7.1E-2
Embryonic heart	2	1.6	5.9E-2
Thyroid carcinoma	2	1.6	7.8E-2

D.

MiR-128 muscle-enriched targets

Gene symbol	Gene name
<i>BMI1</i>	BMI1 polycomb ring finger oncogene
<i>EYA4</i>	eyes absent homolog (Drosophila)
<i>HOXA10</i>	homeobox A10
<i>MEIS2</i>	Meis homeobox 2
<i>MSTN</i>	myostatin
<i>MYH10</i>	myosin, heavy chain 10, non-muscle
<i>NUS1</i>	nuclear undecaprenyl pyrophosphate synthase 1 homolog (S. cerevisiae)
<i>RORA</i>	RAR-related orphan receptor A
<i>RYBP</i>	RING1 and YY1 binding protein
<i>SPRY2</i>	sprouty homolog 2 (Drosophila)

E.

Identity/Similarity (%)

	Gga-EYA4	Hsa-EYA4	Mmu-Eya4	Xtr-eya4
Gga-EYA4	100	94.7/97.1	91.3/93.5	85.8/91.7
Hsa-EYA4		100	93.0/94.7	86.1/92.4
Mmu-Eya4			100	82.7/88.7
Xtr-eya4				100

F.

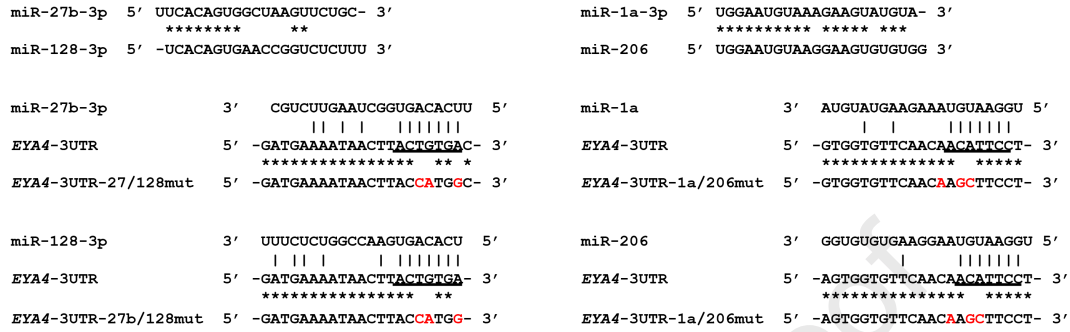
Identity/Similarity (%)

	Gga-EYA1	Gga-EYA2	Gga-EYA3	Gga-EYA4
Gga-EYA1	100	54.5/62.8	46.9/59.9	72.1/82.8
Gga-EYA2		100	46.9/61.0	52.7/63.6
Gga-EYA3			100	48.8/63.3
Gga-EYA4				100

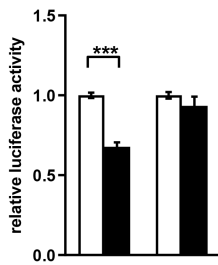
A.



B.

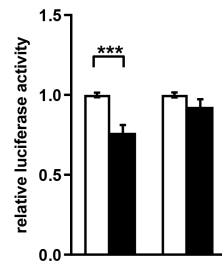


C.



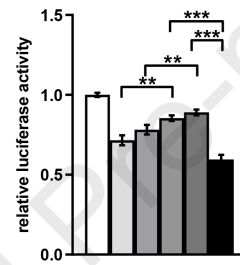
EYA4-3UTR	+	+	-	-
mut-27/128	-	-	+	+
siC	+	-	+	-
si128	-	+	-	+

D.



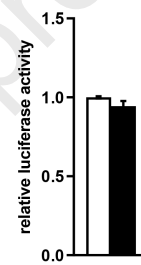
EYA4-3UTR	+	+	-	-
mut-1/206	-	-	+	+
siC	+	-	+	-
si206	-	+	-	+

E.



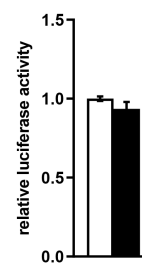
EYA4-3UTR	+	+	+	+	+
mut-1/206	-	-	-	-	-
siC	+	-	+	-	+
si128	-	+	-	+	-
si206	-	-	+	-	+

F.



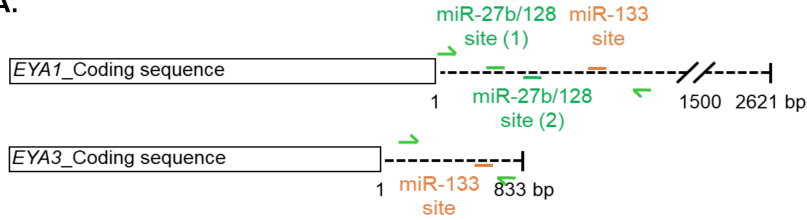
EYA4-3UTR	+	+
mut-27/128	-	-
siC	+	-
si27b	-	+

G.



EYA4-3UTR	+	+
mut-27/128	-	-
siC	+	-
si1a	-	+

A.



B.

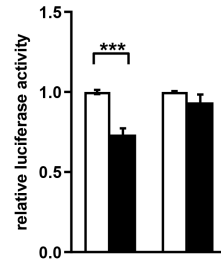
```

miR-133      3'  UGUCGACCAACUCCCCUGGUU  5'
              ||  ||| |||
EYA1-3UTR   5'  -TAGATAAATTTGTCAAGACCAA-  3'
              ***** * *
EYA1-3UTR-133mut 5' -TAGATAAATTTGTCAAGTACCA- 3'

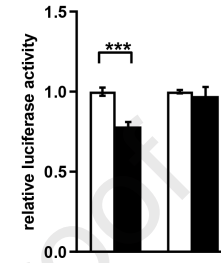
miR-133      3'  UGUCGACCAACUCCCCUGGUU  5'
              ||  ||| |||
EYA3-3UTR   5'  -CTGTTAATGAGCAGGGGATCAT- 3'
              ***** * *
EYA3-3UTR-133mut 5' -CTGTTAATGAGCAGATCTTCAT- 3'

miR-133      3'  UGUCGACCAACUCCCCUGGUU  5'
              ||  ||| |||
EYA4-3UTR   5'  -GGAGGTTGATAGTGGGGACCGC- 3'
              ***** * *
EYA4-3UTR-133mut 5' -GGAGGTTGATAGTGGCTAGCGC- 3'
    
```

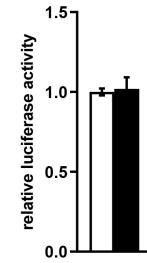
C.



D.



E.



EYA1-3UTR	+	+	-	-	EYA3-3UTR	+	+	-	-	EYA4-3UTR	+	+
mut-133a	-	-	+	+	mut-133a	-	-	+	+	siC	+	-
siC	+	-	+	-	siC	+	-	+	-	si133a	-	+
si133a	-	+	-	+	si133a	-	+	-	+			

F.

```

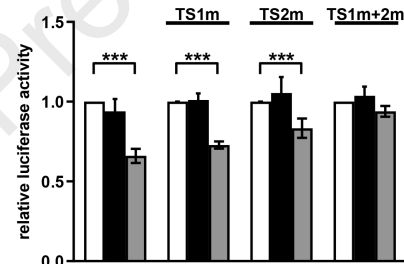
miR-27b-3p   3'  -CGUCUUGAAUCGGUGACACUU  5'
              ||  ||| |||
EYA1-3UTR   5'  CTGTTGACTCTGGTACTGCGAG  3'
              ***** * *
EYA1-3UTR-27/128mut(1) 5' CTGTTGACTCTGGTGGCGCGC 3'

miR-27b-3p   3'  -CGUCUUGAAUCGGUGACACUU  5'
              ||  ||| |||
EYA1-3UTR   5'  AATAAAGGTTGCTACCTGTGAA  3'
              ***** * *
EYA1-3UTR-27/128mut(2) 5' AATAAAGGTTGCTACCGGTACC 3'

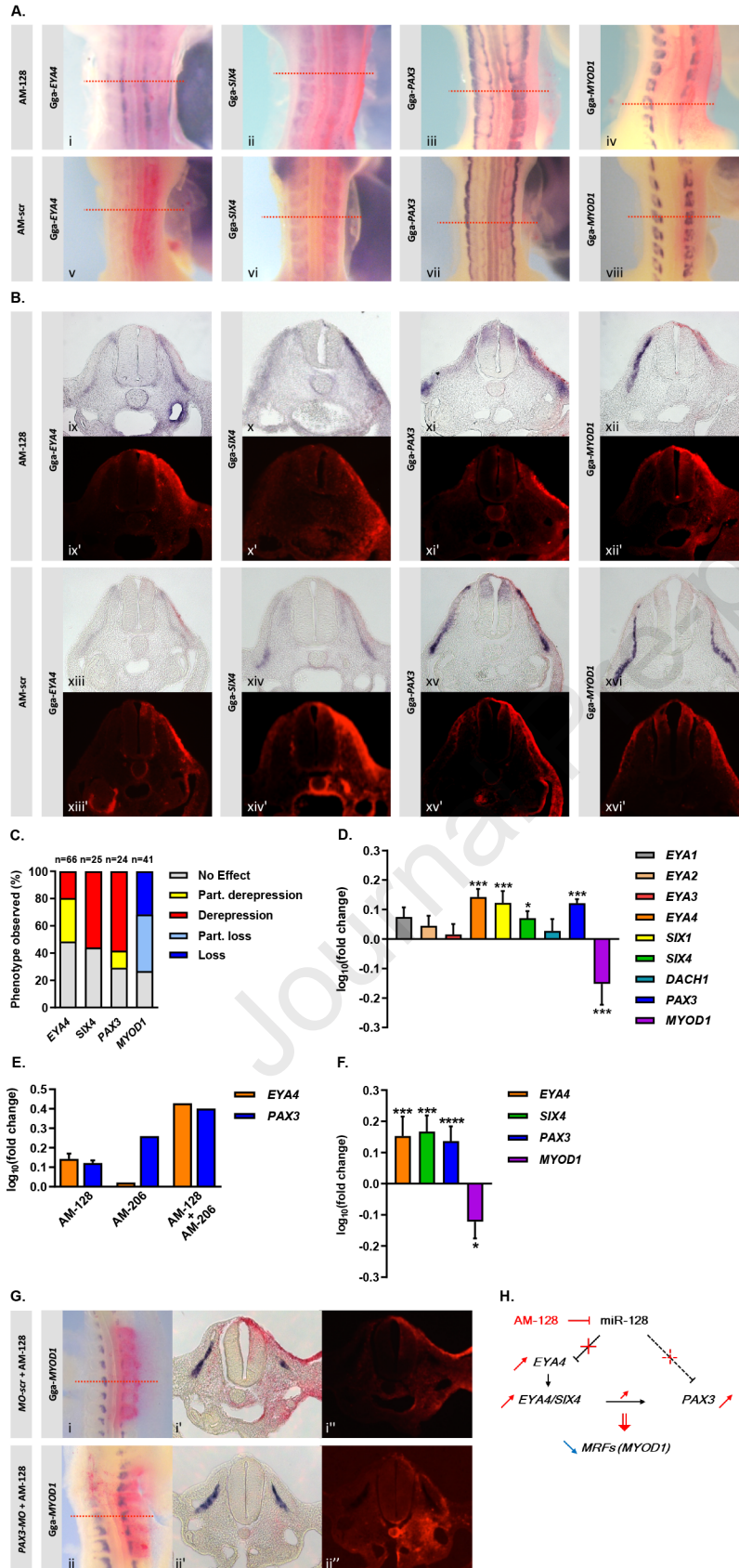
miR-128-3p   3'  UUUCUCUGGCCAAGUGACACU-  5'
              ||  ||| |||
EYA1-3UTR   5'  CTGTTGACTCTGGTACTGCGAG  3'
              ***** * *
EYA1-3UTR-27/128mut(1) 5' CTGTTGACTCTGGTGGCGCGC 3'

miR-128-3p   3'  UUUCUCUGGCCAAGUGACACU-  5'
              ||  ||| |||
EYA1-3UTR   5'  AATAAAGGTTGCTACCTGTGAA  3'
              ***** * *
EYA1-3UTR-27/128mut(2) 5' AATAAAGGTTGCTACCGGTACC 3'
    
```

G.



EYA1-3UTR	+	+	+	-	-	-	-	-	-	-	-
mut-27128 (m1)	-	-	-	+	+	+	-	-	-	-	-
mut-27128 (m2)	-	-	-	-	-	-	+	+	+	-	-
mut-27128 (DM)	-	-	-	-	-	-	-	-	-	+	+
siC	+	-	+	-	+	-	+	-	+	-	-
si27b	-	+	-	-	+	-	-	+	-	-	+
si128	-	-	+	-	-	+	-	-	+	-	-



Highlights

- miR-128 directly targets *EYA4* *in vitro* and *in vivo* in developing somites
- Inhibition of miR-128 inhibits myogenesis indicated by loss of MYOD1 expression
- Inhibition of miR-128 in developing chick somites deregulates expression of EYA4 and other members of the PSED network, including PAX3
- The negative effect of miR-128 knockdown on myogenesis is restored by inhibition of PAX3

Journal Pre-proof